Femtosecond pulse generation in a laser with a nonlinear external resonator

J. Mark,* L. Y. Liu, K. L. Hall, H. A. Haus, and E. P. Ippen

Department of Electrical Engineering and Computer Science, Massachusetts Institute of Technology, Cambridge, Massachusetts 02139

Received August 8, 1988; accepted October 19, 1988

A simple model is presented to describe mode locking in a laser coupled to a nonlinear resonator. It reveals a new mechanism for pulse shortening and shows that shortening does not rely on dispersion in the auxiliary cavity. Experimental results are given to support the basic predictions of the model.

Femtosecond pulse generation is achieved most directly by passive mode locking. At laser wavelengths for which no effective saturable absorber is available, femtosecond pulses can also be produced by nonlinear propagation in an optical fiber, but it is then generally difficult to suppress the uncompressed background completely. The soliton laser of Mollenauer and Stolen[1] solved this problem for a specific case. In their system, $N = 2$ soliton formation in an external fiber provides the pulse shortening that controls the laser. Under different conditions other approaches are possible. Several authors have studied pulse shaping in external resonators theoretically,[2,3] and self-phase modulation alone has been used to obtain mode locking in other laser systems.[4,5] Recently, further experimental research with coupled fiber cavities[6,7] has also indicated that soliton formation is not necessary and that short laser pulses can be achieved even with positive dispersion in the external fiber cavity. In this Letter we present a simple theory that describes how this works. Our theory shows clearly how the relative cavity lengths should be adjusted for optimum pulse shortening and that dispersion is not required for the pulse-shortening process. We then present experimental results obtained in the nonsoliton regime that support predictions of the theory.

Consider a mode-locked laser with part of its output passed through a short length of optical fiber before being reinjected into the main cavity. Such a construction is illustrated in Fig. 1. The path length of the auxiliary cavity is approximately equal to that of the laser cavity, so that the reinjected pulse interferes coherently with the internal pulse. Piezoelectric variation of the auxiliary cavity length controls the phase of this interference. As an example, consider the case in which there is no dispersion in the fiber: the reinjected pulse has the same shape as the internal pulse. Assume further that in the absence of nonlinearity the phase of the reinjected pulse leads that of the internal pulse by some angle between 0 and π; the interference is less than completely additive. Then any self-phase modulation, i.e., nonlinear phase retardation, in the auxiliary cavity will lead to more additive behavior near the peak of the pulse than in the wings. The net effect is that the laser cavity sees the auxiliary cavity as a termination that returns a shorter pulse than is incident upon it. Since the pulse shortening occurs as a result of pulses in the laser and auxiliary cavities interfering additively at the common mirror, we call the use of this mechanism for mode-locking additive-pulse mode locking (APM). The important point is that it works without any shaping of the pulse-amplitude envelope in the nonlinear resonator. It is in fact relatively insensitive to such pulse shaping.

We now consider pulse shaping at the common mirror in a little more detail. The incident and reflected waves are a_1 and b_1 on the laser side and a_2 and b_2 on the auxiliary cavity side. The equations for these wave amplitudes are[8]

$$b_1 = ra_1 + \sqrt{1 - r^2}a_2, \tag{1}$$

$$b_2 = \sqrt{1 - r^2}a_1 - ra_2. \tag{2}$$

Wave $b_2(t)$ travels through the nonlinear medium (we ignore dispersion at first), is attenuated by the factor L (<1), and returns delayed as wave a_2. If the round-trip time equals the period of the pulses, that delay can be suppressed, and one may write

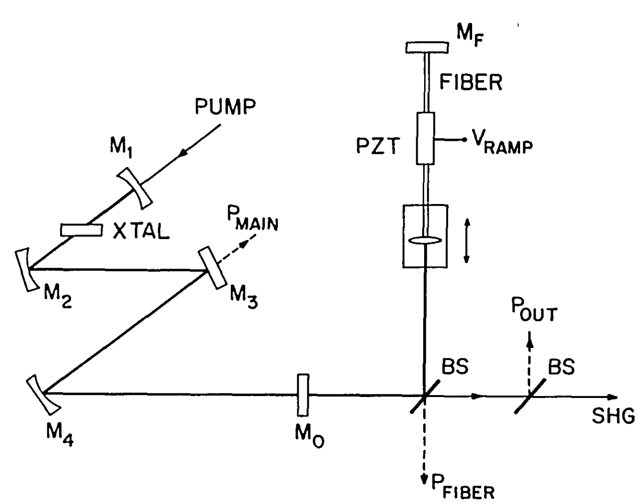

Fig. 1. Experimental configuration with the color-center laser coupled to an external fiber resonator. M's, mirrors; BS's, beam splitters; V_{RAMP}, ramp velocity; SHG, second-harmonic generation; XTAL, F-center crystal.

0146-9592/89/010048-03$2.00/0

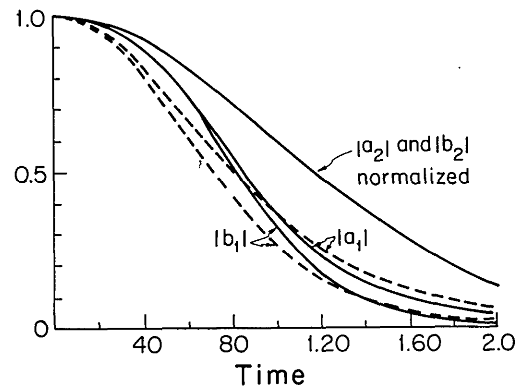

Fig. 2. Incident (a_1) and reflected (b_1) pulse shapes at mirror M_0. The solid curves are for $\phi = 0$, $\kappa = \pi$; the dashed curves are for $\phi = -\pi/2, \kappa = \pi/2$. All pulses are normalized to unity peak amplitude.

$$a_2(t) = L \exp(-j\{\phi + \kappa[|a_2(t)|^2 - |a_2(0)|^2)]\}),$$
$$b_2(t) = L \exp[-j(\phi + \Phi)]b_2(t), \tag{3}$$

where $t = 0$ corresponds to the peak of the pulse and Φ is the phase shift induced by the nonlinearity,

$$\Phi \equiv \kappa[|a_2(t)|^2 - |a_2(0)|^2]. \tag{4}$$

The parameter κ is proportional to the length of the fiber and the nonlinear index. The variable ϕ is the phase shift of the carrier when the (auxiliary) cavity is detuned from antiresonance, the adjustment at which the ratio of energy densities outside and inside the auxiliary cavity is a maximum. Note that the peak phase shift $\kappa|a_2(0)|^2$ has been subtracted from Φ. Thus ϕ includes the phase bias set by the cavity length and a bias due to the peak nonlinear phase shift. By introducing Eqs. (3) into Eqs. (1) and (2) we may then calculate the amplitudes $a_1(t)$ and $b_1(t)$ on the laser side in terms of $a_2(t)$.

For illustration, we assume that a_2 is a Gaussian function of time, $a_2(t) = \exp[-(t^2/2\tau^2)]$. Figure 2 shows the resulting amplitudes of the incident and reflected pulses on the laser side for two cases. The solid curves labeled $|a_1|$ and $|b_1|$ result when the maximum nonlinear phase shift is $\kappa = \pi$ and the phase in the auxiliary cavity is adjusted to give maximum subtraction in the wings of the pulse. This occurs at $\phi = 0$, the case of antiresonance. We see that the reflected pulse $|b_1|$ is shorter than the incident pulse $|a_1|$. Note that we have plotted all pulses normalized to the same amplitude so that the width changes can be observed more clearly. For this case, where $r = 0.8$ and $L = 0.3$, the actual ratios of peak pulse amplitudes $a_1{:}b_1{:}b_2{:}a_2$ are 1:0.94:0.23:0.08.

However, $\phi = 0$ is not the case of best pulse shortening. The dashed curves labeled $|a_1|$ and $|b_1|$ in Fig. 2 are for the case $\phi = -\pi/2$, $\kappa = \pi/2$. Again the peak pulse amplitudes, now in the ratios of 1:0.9:0.32:0.1, have been normalized. Here the shortening is clearly more dramatic. It is also easily understood. Since the nonlinearly phase-shifted pulse is added with a phase shift of $\pi/2$ at the peak, the pulse can start to be in antiphase as soon as one deviates from the peak.

We can show explicitly how the reflection at the peak of the pulse is maximized relative to that of the wings by examining the reflection coefficient

$$\Gamma = \frac{b_1}{a_1} = \frac{1 + \frac{r}{L} e^{j(\phi+\Phi)}}{r + \frac{1}{L} e^{j(\phi+\Phi)}}. \tag{5}$$

If we assume that $L \ll 1$, and Φ is small, then

$$\Gamma = r + L(1 - r^2)e^{-j\phi}(1 - j\Phi). \tag{6}$$

To make $|\Gamma|$ change maximally with a change of Φ, we need $\phi = \pm\pi/2$. It is clear that $\phi = -\pi/2$ causes the reflection to decrease if Φ goes negative. Thus, for $\phi = -\pi/2$,

$$|\Gamma| \simeq r + L(1 - r^2)\Phi. \tag{7}$$

Remember that $\Phi = 0$ at the peak and goes negative in the wings. This shows how the reflection is maximum at the pulse center and then decreases, a simple explanation of the pulse shortening. It also shows clearly why the phase-shift bias of $-\pi/2$ is important. Note, however, that for larger excursions of Φ, the optimum value of ϕ may deviate from $-\pi/2$.

As operation of the APM laser approaches the steady state, the pulse shortening per pass may be expressed as a pulse-shortening velocity.[9] In contrast, however, to the slow-saturable-absorber mode-locked dye laser, where the pulse-shortening velocity is constant for constant pulse energy, here the velocity can actually increase as the pulse duration decreases. Ultimately group-velocity dispersion acts to decrease the pulse-shortening velocity and determines the steady-state pulse duration. Surprisingly, in this regard, the effect of negative (soliton-regime) dispersion is initially more deleterious than that of positive (normal) dispersion, because the phase shifts due to negative dispersion tend to cancel the self-phase modulation directly.

Our APM laser, shown in Fig. 1, is modeled after the soliton laser of Mollenauer and Stolen.[1] The main cavity contains a KCl:Tl^0(1) color-center crystal synchronously pumped at 100 MHz by 100-psec pulses from a cw mode-locked Nd:YAG laser. No bandwidth-limiting tuning plates were used in these experiments. The output mirror, which also serves as the coupling mirror to the auxiliary fiber cavity, has a power reflectivity of 80%. A fraction of the output power was directed into a 40-cm length of dispersion-shifted, non-polarization-preserving fiber by a 50% beam splitter. Including fiber coupling losses, the amplitude attenuation factor L was estimated to be approximately 0.2. For our operating wavelength, $\lambda = 1.52\ \mu$m, pulses propagated in the normal (nonsoliton) dispersion regime with $D = -2$ psec/(nm km). Precise length control of the auxiliary cavity was achieved by stretching the fiber with a piezoelectric element (PZT).

To study APM, we monitored the power level in the main cavity, the output power, and the level of second harmonic generated by the output power as a function of the length of the auxiliary cavity. The laser operated with interferometric stability for periods of several

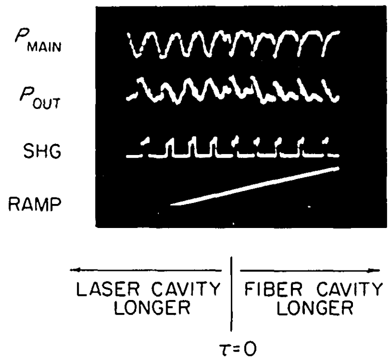

Fig. 3. Variations of internal power, output power, and second-harmonic generation (SHG) as a function of the length of the fiber cavity. Exact cavity match is at $\tau = 0$.

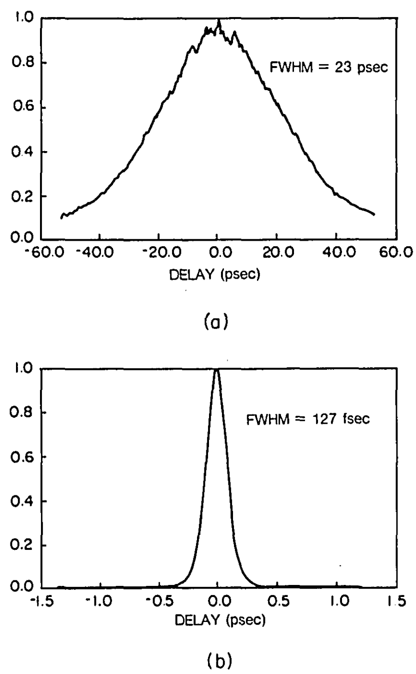

Fig. 4. Intensity autocorrelation traces of the laser (a) without and (b) with an optimally adjusted fiber cavity.

minutes without active stabilization so that these characteristics could be studied simply by applying a voltage ramp to the PZT. Data from such a scan are shown in Fig. 3. In the middle of this scan is a slight discontinuity in the power-versus-length characteristics that we associate with a precise match between the lengths of the two cavities. The variations of main-cavity power (P_{MAIN}) and output power (P_{OUT}) correspond to changes of approximately 10%. Maxima in the main-cavity internal power are points of antiresonance, where the pulse is returned from the auxiliary cavity with zero phase. These points represent effective increases in the output-mirror reflectivity and in our laser occur simultaneously with minima in the output power. The detailed shapes of the curves are more complicated and are related to frequency-pulling effects in the laser. Along with a more detailed theoretical analysis, they will be the subject of a future publication.

The important result of this experiment is the large change in second-harmonic generation observed periodically in the scan. Its amplitude increases by more than two orders of magnitude from minimum to maximum, indicating a dramatic difference in pulse durations. Figure 4 shows intensity autocorrelation measurements taken at the output indicated in Fig. 1 with and without the optimally adjusted auxiliary cavity. APM reduces the pulse width from 23 psec to 127 fsec. Note, with reference to our model, that in the latter case the pulses in the main laser cavity should be even shorter. Average power in both cases was approximately 50 mW. The peak nonlinear phase shift produced in the fiber was estimated to be approximately 10^{-2} rad for 23-psec pulses and approximately $\pi/2$ for 127-fsec pulses. As predicted by our theory, short-pulse operation is achieved only on the negative detuning (shorter-fiber) side of antiresonance. The operating range does center around $-\pi/2$, also in agreement with theory, although operation over almost the entire range from the $-\pi$ to 0 indicates that the APM mechanism is not critically dependent on this phase. Note that pulse shortening is not operative at $\pi/2$, in contrast to reports on the soliton laser.[10,11]

We thank L. Mollenauer for continuing encouragement and help with our color-center laser. E. P. Ippen gratefully acknowledges a stimulating conversation with W. Sibbett. This research was supported in part by Joint Services Electronics Program contract DAAL03-86-K-0002, National Science Foundation grant ECE 84-06290, and U.S. Air Force Office of Sponsored Research grant 85-0213.

The authors are also with the Research Laboratory of Electronics, Massachusetts Institute of Technology, Cambridge, Massachusetts.

* Permanent address, Telecommunications Research Laboratory, Lyngsø Allé 2, DK 2970 Hørsholm, Denmark.

References

1. L. F. Mollenauer and R. H. Stolen, Opt. Lett. **9**, 13 (1984).
2. K. J. Blow and D. Wood, J. Opt. Soc. Am. B **5**, 629 (1988).
3. F. Ouellette and M. Piché, J. Opt. Soc. Am. B **5**, 1228 (1988).
4. L. E. Dahlstrom, Opt. Commun. **5**, 157 (1972).
5. F. Ouellette and M. Piché, Opt. Commun. **60**, 99 (1986).
6. P. N. Kean, R. S. Grant, X. Zhu, D. W. Crust, D. Burns, and W. Sibbett, in *Technical Digest of Conference on Lasers and Electro-Optics* (Optical Society of America, Washington, D.C., 1988), paper PD7.
7. K. J. Blow and B. P. Nelson, in *Proceedings of the Sixth International Conference on Ultrafast Phenomena* (Springer-Verlag, Kyoto, Japan, 1988), paper WC4.
8. H. A. Haus, *Wave and Fields in Optoelectronics* (Prentice-Hall, Englewood Cliffs, N.J., 1984). Here we use a more convenient phase reference for the scattering matrix of the mirror.
9. M. S. Stix and E. P. Ippen, IEEE J. Quantum Electron. **QE-19**, 520 (1983).
10. F. M. Mitschke and L. F. Mollenauer, IEEE J. Quantum Electron. **QE-22**, 2242 (1986).
11. P. A. Belanger, J. Opt. Soc. Am. B **5**, 793 (1988).